J Mater Sci (2007) 42:1797–1808
DOI 10.1007/s10853-006-0973-z

Fatigue limit and crack growth in ultra-fine grain metals produced by severe plastic deformation

A. Vinogradov

Received: 28 June 2006 / Accepted: 15 September 2006 / Published online: 14 December 2006

Abstract The experimental results on fatigue resistance of ultra-fine grain metals produced by severe plastic deformation (SPD) are reviewed with regard to two major characteristics of cyclic damage initiation and failure—fatigue limit and fatigue crack growth rate. The fatigue limit benefits considerably from grain refinement down to submicrocrystalline scale. Factors affecting the fatigue limit are discussed in the light of SPD-processing and resultant ultra-fine grain structure. Contrasting with the fatigue limit, the fatigue crack growth threshold deteriorates after SPD in comparison to that of ordinary polycrystals. Possible mechanisms of fatigue crack initiation and propagation are discussed and the guidelines for manufacturing are provided towards enhancement and optimization of fatigue performance.

Introduction

Fatigue properties of ultra-fine grained (UFG) materials, having the grain dimensions in the sub-micron and nanoscopic range, are of considerable interest. Tremendous improvement of the yield stress σ_y and tensile strength σ_{UTS} after severe plastic deformation (SPD) has been demonstrated in numerous publications after the early work by Segal et al. [1, 2] who proposed an equal-channel angular pressing (ECAP) technique for intensive strain hardening and structure refinement of bulk samples. Traditionally, total fatigue life of a smooth body is divided into two stages—the stage prior to crack initiation and the stage of crack propagation. In high-cycle fatigue (HCF) at relatively small strain amplitudes, the crack initiation stage dominates most of fatigue life whereas low-cycle fatigue (LCF) is associated mostly with the crack propagation, which occurs at relatively large strains [3]. The terms ''high strain'' and ''low strain'' fatigue are rather conventional because the influence of strain magnitude can be significantly different for different materials. For example, little plastic strains which are crucial for brittle materials may be far too low to cause any damage in ductile ones. It is however possible to distinguish quantitatively between the high and low plastic strain amplitudes if the total life fatigue diagram is considered when the number of reversals to failure is plotted versus the total strain amplitude as has been discussed repeatedly in the literature, cf. [4–8]. The transition point can be determined rather rigorously between the two branches of the fatigue diagram in terms of Coffin-Manson and Basquin parameters [3] of cyclic life, i.e., between (i) the low strain region when the elastic part of the cyclic hysteresis loop is dominant and when fatigue life is controlled by the strength of materials primarily and (ii) high strains, when the plastic part of the hysteresis is prominent so that the ductility governs the fatigue life. Hence, the resistance to crack initiation naturally requires strength while the tolerance to the crack advance requires ductility. The most promising feature of SPD materials, which suggests the possibility of obtaining significantly enhanced fatigue properties, is associated with a combination of high strength and good ductility in

A. Vinogradov (✉)
Department of Intelligent Materials Engineering,
Osaka City University, Osaka 558-8585, Japan
e-mail: alexei@imat.eng.osaka-cu.ac.jp

the nano-structured state [9–11]. The primary characteristic of fatigue in the high cycle regime is the fatigue limit σ_f, i.e., the stress amplitude below which no fatigue occurs in symmetric push-pull testing until the number of cycles to failure N_f is less than a certain number conventionally taken as 10^7. It has long been realized that σ_f correlates with the yield stress or the ultimate tensile strength. As a rule of thumb for materials processing it is commonly suggested that high strength and, consequently, strengthening to the maximum extent strength is desired for achieving the ultimate high-cyclic fatigue performance and highest fatigue limit. Since SPD offers a spectacular strengthening effect to materials, the enhancement of fatigue properties at small strain amplitudes is reasonably anticipated and is achieved indeed as seen in Fig. 1 where the correlation between the monotonic and cyclic strength is illustrated. The effect of strengthening is however not that straightforward, depending on the slip type. For instance, wavy slip materials like copper do not exhibit a strong dependence of σ_f on either grain size [12–14] or initial dislocation density varied by the amount of pre-strain [3, 15], cf. Fig. 2.

We will first consider the fatigue crack nucleation and propagation in smooth UFG specimens at both small and high applied stresses, i.e., in high- and low-cycle fatigue, respectively. Then we shall discuss the fatigue crack resistance in notched UFG bodies with emphasize on phenomenology of fatigue crack growth behavior and the influence of the microstructure. Limiting ourselves to pure and single phase materials,

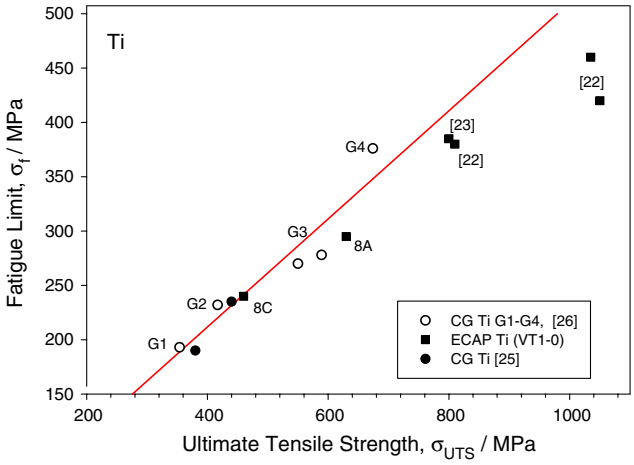

Fig. 1 Correlation between the tensile strength and fatigue limit in commercial purity Ti. G1, G2, G3 and G4 stand for the standard Grade ASM designation of Ti products. Noticeable deviation is observed for the highest strength SPD-manufactured Ti (ECAP followed by cold deformation) from the value expected from the regression line, which was produced from data for CG Ti

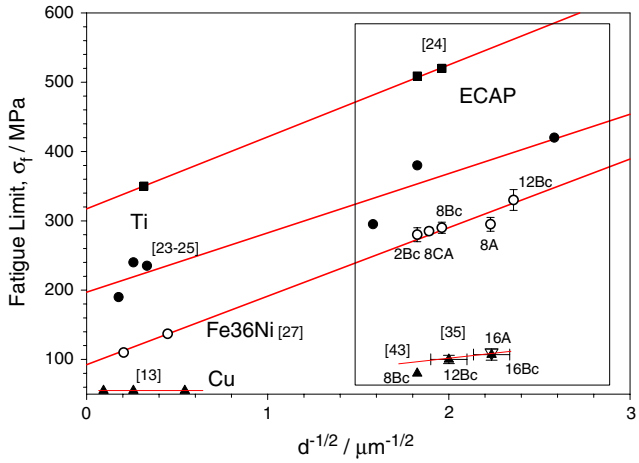

Fig. 2 Dependence of fatigue limit on the grain size for CG and UFG materials with different type crystal lattice and slip. The results from ref. [16] are plotted for the number of cycles to failure $N_f = 10^6$ under zero-tension ($R = 0$) loading conditions, i.e., this explains the much higher fatigue limit than that reported in [17]. Data for ECAP Cu pressed to 16 passed by routes A and Bc, i.e., samples 16A and 16Bc, respectively, and for ECAP Fe36Ni 8Bc and 8A are obtained in the present work

let us review briefly the factors affecting the fatigue limit and the fatigue threshold. These can be divided into three main groups:

1. *material and structure related factors* such as (a) type of dislocation slip, (b) grain size, (c) dislocation density and distribution, (d) texture, (e) residual stresses;
2. *loading factors*: (a) stress ratio, (b) mean stress, (c) frequency, (d) temperature, (e) environment;
3. *design factors*: (a) specimen shape and dimensions, (b) surface conditions such as finishing and hardening/softening treatment of the surface layer.

Since experimental data are not readily available yet to address all these issues for UFG materials we shall discuss the fatigue limit in the small strain (high-cycle) region and fatigue crack resistance in terms of threshold and crack growth rate. The reviews and original articles regarding the effect of ultra-fine grain size and SPD processing on the cyclic response and the fatigue behavior under high applied strains (low-cycle regime) can be found elsewhere (see [6, 8] and references therein, for example).

Effect of grain size and SPD on fatigue limit

The effect of grain size on cyclic plasticity and fatigue life has been in focus of many investigations [14, 18, 19]. Two major conclusions can be drawn:

(i) The fatigue limit of pure f.c.c. metals with relatively high stacking fault energy and wavy slip behavior is not affected by the grain size (compare Fig. 2, $0 < d^{-1/2} < 0.3$ corresponding to conventional Cu).

(ii) The fatigue strength of materials exhibiting planar slip increases with decreasing grain size and follows the Hall–Petch relationship, shown below, in the same way as the yield stress in conventional polycrystals:

$$\sigma_f = \sigma_{0f} + K_f d^{-1/2} \quad (1)$$

where σ_{0f} and K_f empiric materials properties. The Hall–Petch type behavior of the fatigue limit in metals with the grain size reduced to the sub-micron scale after ECAP is illustrated in Fig. 2 for Ti and Fe36Ni alloy. The first conclusion highlights the slip type as one of the most important material characteristics that controls the fatigue behavior. During cyclic deformation, the wavy slip materials form a well-defined cell structure with the cell size being dependent upon the saturation stress and independent of the preliminary strain history [3, 12–15, 18–20]. Materials with a planar slip do not form a cell structure and dislocations are arranged in planar arrays extending across a grain. Tompson and Backofen [13] using pure copper (wavy slip) and α-brass (planar slip) have demonstrated convincingly that grain size has a more pronounced effect on the fatigue behavior of planar slip materials. Although this view can be extended to UFG metals in that the other than wavy-slip materials are more susceptible to improvement of fatigue limit [4], the striking result of grain refinement down to submicrocrystalline scale is that even such typical representatives of wavy-slip materials as Cu and Al exhibit prominent rise in their fatigue performance after ECAP. The results on copper vary notably from modest (of 80 MPa [6]) to high (150 MPa [21]) σ_f enhancement, depending, possibly, on impurity content and fabrication (the effect of processing will be discussed below). A very strong enhancement of fatigue limit has been reported for the CuCrZr alloy [22] and α-brass [23] exhibiting planar slip. Similarly, pure titanium appears to be prone to considerable HCF properties enhancement [16, 17, 24] in comparison with its ordinary CG counterpart [25, 26]. Indeed, Fig. 1 and 2 illustrate the increase of σ_f after ECAP. One can notice, however, that the sample having the highest σ_{UTS} value of 1,150 MPa and the finest fibrous-like grain structure obtained in commercial purity Ti in the course of ECAP followed by cold rolling reveals some deviation from the value expected from the simple $\sigma_f - \sigma_{UTS}$ or $\sigma_f - \sigma_{0.2}$ proportionality. This result is not surprising and expected from the behavior of other high strength materials. Although unknown precisely, several reasons can account for it: (i) appearance of undocumented stress risers such as micro-cracks which are often beyond the control during SPD (this reason is believed to be most significant), (ii) structural instability after SPD, (iii) stronger influence of environment in the UFG state after SPD, etc.

We should underline that the amount of the strain imposed or the number of ECAP passes exerts usually a strong positive effect on the fatigue limit. Figure 2 illustrates this point for the ECAP Fe36Ni alloy processed to 2, 8 and 12 passes [27]. On the other hand, the strain path has been proven to have modest effect on the structure and tensile behaviour [28] as well as on the LCF [29, 30] properties if the number of passes is sufficiently large, depending on material. Some little effect of the processing route on HCF is visible in Fig. 2 for Fe36Ni alloy processed by routes A, B_C and CA to 8 passes at room temperature: route A appears to have the finest grain boundary spacing and the slightly higher fatigue limit. Nevertheless, the results of σ_f evaluation scatter considerably. The structural distinction between differently processed samples diminishes when the number of passes increases to 12 or 16. It is therefore plausible to expect that the effect of strain path on the mechanical behaviour reduces with the amount of pre-strain in SPD manufacturing. Among the other processing parameters, which are of primary importance for the HCF performance, we should mention the encouraging influence of the hydrostatic pressure giving rise to increasing shear uniformity and to reducing local stress concentrations during fabrication. For instance, Lapovok et al. [31] have shown that ECAP with controllable back pressure can be effective for enhancement of fatigue life in both LCF and HCF of the 2124 Al-alloy.

The independence of the grain size in coarse grain (CG) wavy slip f.c.c. metals is related to specific dislocation structures as cells, labyrinths, ladders, veins and persistent slip bands (PSBs) formed during cycling [3, 14, 15, 32]. Since the typical grain/cell size in the SPD metals of 100–300 nm is smaller than the typical scales of fatigue structures associated with the above mentioned dislocation arrangements in CG metals (~500 nm), exceptions to the classical rules are anticipated, giving rise to the improvement of fatigue limit with grain refinement and strain hardening in wavy slip materials as well.

Although, modeling of fatigue limit is far for from its completeness even in conventional CG materials, a brief discussion on physical reasons for limiting the cyclic performance of pure and single-phase materials seems to be in place with the possible implications for UFG materials. Lukáš and Kunz [33] reviewed recently the results of TEM observations in high-cyclic fatigue regime and argued that cyclic plastic deformation at low strains occurs rather inhomogeneously in such a way that plastic deformation does not occur in all grains in HCF region, while in LCF region all grains deform plastically by multiple slip leading to the distinguished dislocations structures such as cells and PSBs. This constitutes one of the basic differences between LCF and HCF regions. Moreover, the same authors indicated that activity of one slip system (a consequence of which is the vein structure) is often sufficient for accommodation of very low plastic strains imposed (say as low as those near the fatigue limit). Since the grains at the surface are less constrained than the interior grains and since the surface offers more potential local stress risers than the interior, plastic deformation often occurs easier at the surface so that it might be plausible to suppose that at very low cyclic strain amplitudes the slip occurs only in some grains at the specimen surface. Hence, the particular significance of the surface structure and surface conditions for HCF is anticipated. The so-called bi-modal grain structure which is often observed in SPD-produced materials after low-temperature annealing has been shown to be beneficial for LCF properties due to gain of ductility [11]. However, it has not been explored yet if such a structure would help to enhance the fatigue life in HCF and to improve the fatigue limit. The question arises actually with regard to both crack initiation and propagation in the bi-modal structure. The major concern occurs because the bi-modal structure would promote the inhomogeneity of slip since the annealed grains would yield first, giving rise possibly to early PSB formation in larger grains at the PSB threshold stress, leading to the ''classic'' crack nucleation scenario in the fatigue intrusions associated with PSBs or at the or grain boundary/PSB interface.

Potentially, a small grain size can result in more homogeneous deformation, which can retard crack nucleation by reducing stress concentrations and ultimately raise the fatigue limit of the material. Although the precise mechanism of cyclic degradation at small imposed strains as well as the nature of the fatigue limit in UFG structures remains undisclosed yet, the considerable enhancement in the σ_f value after ECAP has often been reported. Figure 2 illustrates the progressive increase in the σ_f value with the amount of strain or the number of ECA-passes. Furthermore, similarly to that of planar slip f.c.c. Fe36Ni alloy and of h.c.p. Ti, the fatigue limit for ECAP Cu appears to be sensitive to the pre-strain history, i.e., to the amount of strain imposed onto the sample during manufacturing, Fig. 2. It has been reported that the fatigue limit obeys the Hall–Petch relationship with decreasing grain size to the submicrocrystalline scale in the same way as the ultimate tensile strength σ_{UTS} [17]. An estimate of the stress required for dislocation multiplication by Frank-Reed mechanism (where the source-length is assumed to be one half the grain size) in the UFG materials would give $\tau \geq 2\mu b/d$, which yields for UFG copper (having typically $d = 200$ nm, $\mu = 45$ GPa and $b = 2.5 \times 10^{-10}$ m) the normal stress $\sigma = M\tau \approx 360$ MPa which compares favorably with the conventional yield stress $\sigma_{0.2}$ for ECAP Cu, but is far too large for any reasonable estimates of the fatigue limit. Such a high stress indicates that dislocation activity within nano- and ultra-fine grains is expected to be difficult (although possible). However, the grain boundaries, particularly the so-called non-equilibrium grain boundaries having long-range stress fields, remain to be potential sources for dislocation multiplication. For example, the AFM observations [34, 35] show that the slip lines activate primarily near the grain boundaries just above the yield point in UFG Ni manufactured by ECAP. Returning to the last estimate of the dislocation multiplication stress, one should bear in mind that the applicability of average materials characteristics for assessing the fatigue limit is not justified in general case. To the contrast, a ''weakest link'' concept can be applied. Apparently, the occurrence and variation of microstresses play an important role in initiation of fatigue damage identified as a highly localized process associated with the ''weakest link'' of the material. In this sense, a rather broad distribution of grain/cell sizes in SPD materials may exert a considerable effect on fatigue limit because the larger grains would tend to yield at lower stresses. In other words, the distribution of microstresses and their peak values seem to be important for fatigue crack initiation. At this point we face a contradiction. On one hand it is apparent that the fatigue limit correlates with the materials strength or yield stress (Fig. 1), i.e., the high strength is desirable to impede plastic deformation, which would inevitably lead to crack formation. On the other hand, high microstresses are undesirable since they increase the local loading on the material, resulting from the sum of external and internal load. If such high microstresses are unevenly distributed over the specimen volume, as is expected after SPD where the gradients of plastic flow and shear banding are quite

common (e.g., [36]), they can serve as stress risers reducing dramatically both the fatigue limit and the fatigue threshold from their potentially higher values.

In a classic dislocation approach, Finney and Laird [37] have pointed out that there can be no mechanism for fatigue fracture if PSBs are absent. Laird [38] has considered the stress-strain requirements for PSB formation in copper single crystals. He associated the plateau shear stress $\tau = 8$ MPa, which is the PSB-threshold stress and which has been proven virtually independent of the strain rate, grain size and pre-load history, with the endurance limit for copper provided that the appropriate Taylor, Sachs or Schmidt orientation factor applies (compare also [39–41]). Indeed, the fatigue limit for CG Cu shown in Fig. 2 compares favorably with the PSB threshold if the Taylor orientation factor of 3.06 is adopted. Hence, PSBs are obvious prerequisites for crack nucleation in single- and polycrystalline materials [18, 41]. Essmann, Gösselle and Mughrabi [42] have developed a model for surface roughening and crack nucleation, assuming the annihilation of dislocations within the slip bands to be responsible for slip irreversibility. The same or any other PSB-based model is unlikely applicable to UFG materials in HCF deformation since no evidence for PSB formation has been found so far under very low strains (let us, however, notice that at high strains in LCF the PSB-like ladder structures have been reproducibly observed in pure ECAP metals such as Cu due to instability of their UFG structure tending to coarsen under applied load [5–8, 43–45]). However, the rational point of this model is that without annihilation the to-and-fro motion of dislocations within the grains in a flip-flop manner would be reversible and no surface topography alternations would be anticipated. Observations of the surface topography by means of atomic force microscopy (AFM) in LCF regime however reveal a clearly pronounced slip relief as illustrated in Fig. 3 for ECAP Fe36Ni alloy (no similar observations have been performed on UFG metals after HCF so far, to our knowledge). The image force acting on a dislocation line bowing out from grain boundaries under applied far-field stresses can be considered as one of potent candidates for surface slip irreversibility in UFG and nano-structured materials.

One more aspect is worth noting with regard to the fatigue life-controlling factors in HCF regime. Mughrabi has recently underlined the role of diffusion-controlled effects in the ultra-high cycle fatigue damage [46]. He argued that the mean diffusion path x given as

$$x \sim \sqrt{D \cdot N_f / v} \tag{2}$$

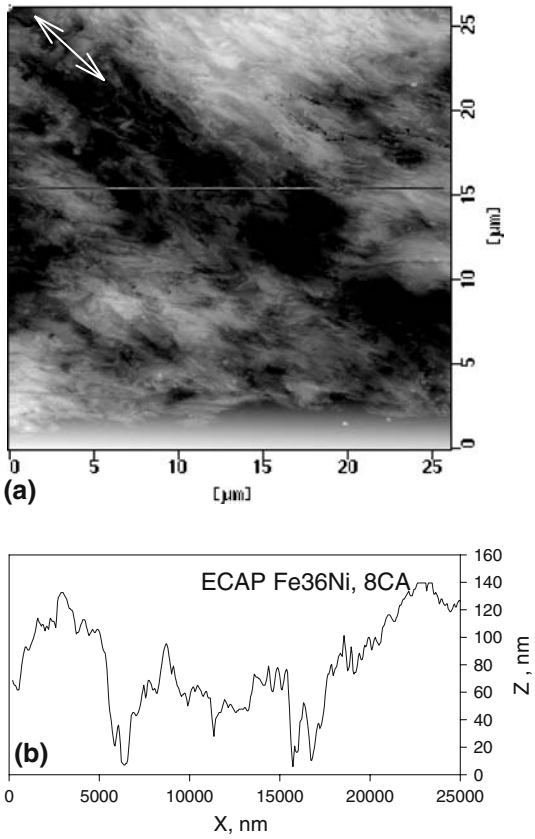

Fig. 3 Surface topography revealing extrusions and intrusions after cyclic loading of ECAP Fe36Ni alloy (route CA, 8 passes) at $\Delta\varepsilon_{pl}/2 = 1 \times 10^{-3}$ for $N = 100$ cycles: (**a**) AFM image; (**b**) surface profile measured along the line marked on (**a**). Loading axis is vertical. An arrow indicates a shear plane in the last pressing operation

where D is the diffusion coefficient, N_f is the number of cycles to failure and v is the frequency of loading, could be quite considerable in the gigacycle region, emphasizing thereby the significance of time-dependent factors in fatigue. Recalling specific properties of SPD-manufactured materials, the remarkable increase of the grain boundary diffusion coefficient by 2–4 orders of magnitude has been reported repeatedly [9, 46]. Assuming the grain boundary diffusion coefficient D for nanotructured and SPD-processed UFG metals to be in a range of 10^{-16}–10^{-19} m^2/s [47] and taking for HCF $N_f = 10^7$ and testing frequency of 10 Hz, one estimates x to be of 3×10^{-7}–10^{-5} m which is comparable or exceeding the characteristic grain size. It is therefore plausible to suppose that the fatigue limit can be to some extent, if not entirely, affected by diffusion-controlled processes. The time/frequency dependence of fatigue life should be anticipated accordingly. It is timely to notice, that the strong frequency dependence has been reported indeed in the LCF testing of Fe-36Ni alloy [27], Cu an Al [48, 49] so that the fatigue life decreased with frequency reduction

Table 1 Mechanical properties and crack growth characteristics of ECAP materials

Sample	σ_y, MPa	σ_{UTS}, MPa	δ, %	σ_f, MPa	ΔK_{th}, MPa × $m^{1/2}$	C, mm/cycle	m
Cu CG (d = 11 μm)				56		7.9×10^{-10}	4.2
Cu CG (d = 15 μm) [52]	65			-	4.5***	5.3×10^{-9}	3.5
Cu UFG ECAP 4Bc	310	430	12	80	4.4	1.2×10^{-7}	2.1
Cu UFG ECAP 12 Bc [53]	480	512	17	115	2.4	8.3×10^{-8}	2.0
Cu UFG ECAP 16 Bc	350	413	15	110	2.4	8.5×10^{-8}	2.1
Cu UFG ECAP 16 A	350	420	14	115	2.7	1.2×10^{-8}	2.1
Cu0.5Cr0.08Zr CG	300	350	12	120	1.5		
# ECAP 8 Bc [54]	470	480	19	170		2.4×10^{-7}	2.0
6061 Al–Mg CG [55]	150	270	48	35*	4.5	6.3×10^{-9}	4.2**
# ECAP 4Bc [55]	380	420	22	80*	3.8	4.1×10^{-9}	4.4**
5056 Al–Mg CG [56]	122	288	43	116	5.7	3.9×10^{-9}	4.4
# ECAP 4Bc [56]	280	340	25	116	4.2	7.5×10^{-8}	3.2

*Data obtained for R = 0, all others are for R = –1

**Data obtained after calculations by the least square liner fit of the original graphs plotted in ref. [55]

***Data obtained for R = 0.5, all others are for R = 0.1

as expected from the last formulae for the same critical diffusion path. To the contrast, Kunz et al. [21] have reported no frequency effect on the fatigue limit of ECAP Cu, leaving the question about the role of diffusion-controlled processes in fatigue open. Comparing the results by Kunz et al. with other relevant data for fatigue of UFG Cu, one should bear in mind lower purity (99.9%) and greater grain size (of 670 nm) of the samples used in [21]. Closing this brief discussion on the role of time-dependent processes in fatigue we should not forget about the environmental effects which are known to be crucial for fatigue life and fatigue limit. The role of environment in fatigue of UFG and nano-materials has not been investigated yet to our knowledge. Yamasaki et al. [50] have demonstrated notably enhanced fatigue life of ECAP Cu under corrosion fatigue during testing at constant plastic strain amplitudes ranging between 3×10^{-4} and 5×10^{-3} in an aggressive Livingston solution. Yamasaki [51] has also shown that the corrosion fatigue threshold for crack propagation also benefits greatly from grain refinement via ECAP. However, the effect of environment on fatigue of SPD-manufactured materials still cannot be rationalized from the data presently available and this issue deserves special attention in future work.

Effect of SPD on fatigue crack growth

The fatigue life assessment of smooth bodies delivers only indirect information regarding resistance to flaws either preexisting or forming in the course of cycling. Comprehensive understanding of fatigue properties requires evaluation of the fatigue crack growth. Although many features associated with fatigue of smooth UFG samples have been disclosed and understood [4, 8, 35, 48, 49] the crack growth behavior remains to be least studied among other mechanical properties. The attention to fatigue crack propagation in UFG and nano-structured materials tends to increase with recent development of processing capabilities of producing the samples large enough for machining the standard compact tension (CT) or center-cracked-tension (CCT) specimens with dimensions as prescribed by the ASTM standards for crack growth testing. The subsize specimen testing is also possible with caution and measures undertaking to comply with standard requirements and accuracy of crack length evaluation. Some presently available results on the crack growth rate in SPD-produced metals are summarized in Table 1. Perhaps, the first attempt to evaluate the crack growth resistance using the CT specimens was performed by Vinogradov et al. [56] on the non-heat treatable ECAP 5056 Al–Mg alloy. The kinetic diagram showing the crack growth rate da/dN versus the stress intensity factor range ΔK

$$\Delta K = Y \Delta\sigma \sqrt{\pi a} \tag{3}$$

(where Y is the geometrical factor dependent upon the specimen and crack geometry and $\Delta\sigma = \sigma_{max} - \sigma_{min}$ is the applied stress range, a is the crack length) for a given stress ratio $R = \sigma_{min}/\sigma_{max}$ and environment is used commonly to quantify the fatigue crack growth behavior. The da/dN versus ΔK plot for UFG materials [53–55, 57, 58], Figs. 4 and 5, exhibits the same stages of crack propagation as those well-known for conventional poly-crystals, i.e., (1) a stage of slow crack advance in the near threshold region, (2) an intermediate stage and (3) the stage of unstable crack growth at high ΔK values. On the stage 2 of a stable crack propagation the Paris relationship

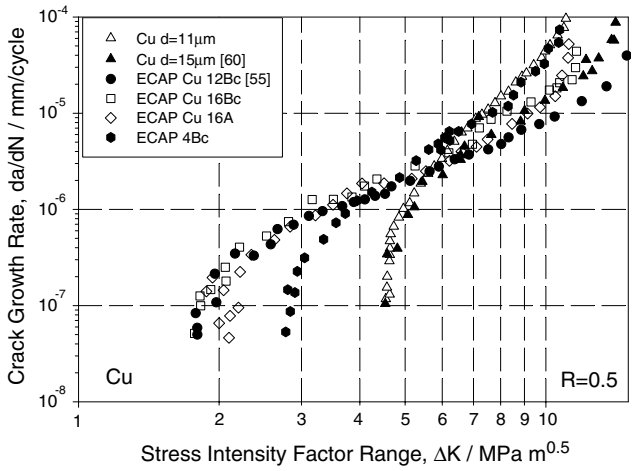

Fig. 4 Fatigue crack growth rate in UFG ECAP copper. Data for conventional CG Cu are plotted for comparison

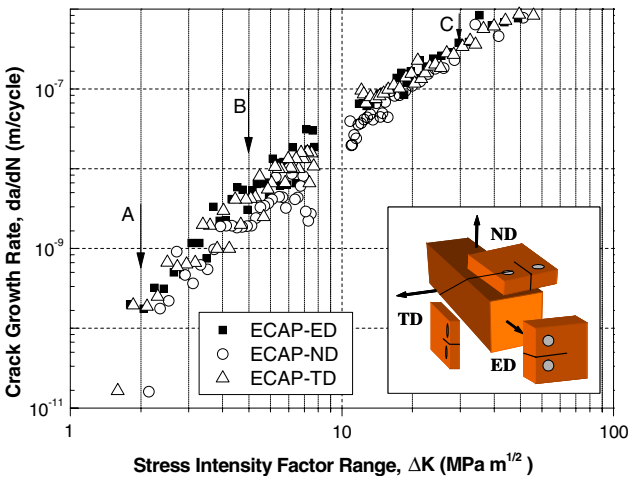

Fig. 5 Fatigue crack growth rate in UFG Cu–0.8Cr–0.05Zr alloy produced by ECAP (8 passes via route Bc, after [54, 58]); ED—extrusion direction, TD—transverse direction, ND—normal direction

$$\frac{da}{dN} = C(\Delta K)^m \tag{4}$$

(with C and m—materials properties) applies. It was found that the fatigue threshold ΔK_{th} decreased after ECAP of a non-heat treatable 5056 Al–Mg alloy [51]. Chung et al. demonstrated very similar results for the UFG 6061 Al-alloy [55] and UFG ECAP low carbon steel [57]. It has been shown that the crack growth rate in the near threshold region is higher in the UFG state than in the ordinary polycrystalline state however the picture is opposite at relatively high stress intensity factor increments ΔK, i.e., da/dN in UFG metals is smaller on the intermediate fatigue stage. The lower crack growth resistance in the near threshold regime was attributed to a less tortuous crack path, which was supposed to be intergranular in the UFG structure. It is worth noticing, Fig. 4, that the processing route does not affect strongly the ΔK_{th} value (the sample produced by route A shows slightly higher ΔK_{th} value than that produced by route Bc) while there is a trend towards ΔK_{th} reduction with increasing number of pressing (compare data for 4Bc and 16Bc samples, for example).

The uniformity of UFG structure after ECAP with the number of pressing of 8 via route Bc results in a similar crack growth behavior regardless of the CT specimen orientation with respect to the billet axes [54], showing no considerable difference in the crack growth rate or fatigue threshold for the samples shaped from different sections of the billet, i.e., the effect of texture on eth crack growth appears to be negligible.

It has long been established in the fracture mechanics approach that the transition from the near-threshold slow crack growth regime to the intermediate fatigue stage is accompanied by a transition in the crack behavior from being strongly structure sensitive to structure insensitive. Such a transition is often observed when the crack tip cyclic plastic zone r_{cp}, which is estimated as

$$r_{cp} = \lambda\left(\frac{\Delta K}{2\sigma_y'}\right)^2 \tag{5}$$

where λ is the numerical factor of the order of $1/\pi$ and σ_y' is the cyclic yield stress determined from the cyclic stress-strain curve (CSSC), becomes of the same order as the grain size d [3, 59]. If the stress intensity factor range corresponding to the transition point is denoted as ΔK_T, the last equation yields a transition criterion $r_{cp}(\Delta K_T) \approx d$. However, estimations of a reverse plastic zone radius r_{cp} at the transition point return a r_{cp} value for the materials tested (Cu, 5056 and 6161 Al-alloys) which is significantly greater than the average grain size d. For example, taking for A5056 Al–Mg alloy $\sigma_y' = 280$ MPa and the threshold $\Delta K = \Delta K_{th} = 4.3$ MPa·m$^{1/2}$ (Table 1) [56] one obtains $r_{cp} = 7$–8 μm that is considerably larger than $d = 0.3$–0.4 μm. This suggests that a large number of neighboring grains may be involved into crack tip plasticity, even near threshold. The Eq. (5) at the transition point can be simply rearranged as

$$\Delta K_T \sim \sigma_y'\sqrt{d^*} \tag{6}$$

with d^* a characteristic scale of a materials structural unit responsible for fracture (grain size, sub-grain or

cell size, particle size, etc.), which predicts ΔK_T to be increasing with d, which is observed in low-carbon steels, for example [3, 59]. Assuming the threshold ΔK_{th} approximately equals ΔK_T, the last relationship is often written in a more general, but less transparent and less argued form as

$$\Delta K_{th} = A + B\sqrt{d^*} \tag{7}$$

with A and B materials constants. In many empiric models, B is taken to be equal to the fatigue limit so that the last expression takes a form $\Delta K_{th} = \sigma_f\sqrt{\pi d*}$ (cf. [60] for example). Observations reported in [31, 32, 40, 61] as well as in the present work show the reduced ΔK_{th} in UFG metals processed by SPD which qualitatively agrees with (6) and (7). However, if Eqs. (6–7) were valid for these materials, a shift of ΔK_{th} to smaller magnitudes (of 1 MPa·m$^{1/2}$ or less in the 5,065 Al–alloy, for example) should be expected, which was far below the observed values of 4–4.5 MPa·m$^{1/2}$. These observations cast some doubt on the applicability of an over-simplified plastic zone size concept to explanation the fatigue threshold behavior in these materials. Contradictory behavior is also well-know in CG materials. Higo et al. [52] have performed a systematic investigation of the ΔK_{th} and da/dN dependence on the grain size and the $\sigma_{0.1}$ yield stress in Cu and Cu–Al alloy with different Al content, i.e., with different stacking fault energy ranged between 5 mJ m^{-2} and 45 mJ m^{-2} approximately. In contrast with the linear behavior of Eq. (7), they have experimentally observed that the propagation rates were slower in the fine-grained materials and da/dN varied linearly with $d^{-1/2}$ in the same manner as the $\sigma_{0.1}$ yield stress, i.e., followed the Hall–Petch relationship, which is opposite to Eqs. (6 and 7). These effects were pronounced in alloys with higher Al content, i.e., in planar slip metals were we noticed that a stronger dependence of fatigue life on the grain size is expected. Thus, it is shown that although the fatigue crack growth behavior in UFG metals reveals some similarity to that of conventional polycrystals, the quantitative explanation of the fatigue threshold reduction as well as the reduction of the crack growth rate at relatively high ΔK is not straightforward. Nevertheless, some efforts are worth making with account for structural features of SPD-manufactured materials.

Many ductile b.c.c. and f.c.c. metals with relatively high stacking fault energy show a predisposition for cell formation during cyclic deformation. Morphologies of dislocation cell structures in front of the fatigue crack tip were reported to be similar so some extent to those found in the LCF test. Figure 6 illustrates a typical cell structure near the edges of the fatigue crack growing in a CG Cu polycrystal. During fatigue crack propagation, the operating stress at crack tip is high enough, particularly at the maximum applied load, to activate many slip systems and trigger the mechanisms of fatigue resembling those at high-strain LCF. Lukas et al. [61, 62] have connected the size of the dislocation cells produced by deformation at the fatigue crack tip with the crack tip stress amplitude. Huang et al. [63] have found that regardless of the plastic strain amplitudes, the average diameter of the dislocation cell in front of the crack tip in Cu is about 0.7 μm. Hence, once the low-energy dislocation cell configuration has formed, the prerequisites exist for both crack initiation and/or propagation so that the cell structure can be generally considered as a ''critical'' structure for fatigue. In account of these observations Lukas and Gerberich [64] proposed a model which utilizes a stable dislocation substructure, i.e., the cell structure that evolves in the vicinity of the crack tip, in order to deduce the effect of the grain size on fatigue threshold. Assuming the cell boundaries are not penetrable for gliding dislocations it was suggested that the fatigue threshold was controlled by the average glide distance of dislocations which was limited by the cell size as illustrated schematically in Fig. 7. Relating the local plastic strain at the crack tip region to the plastic strain in the slip band emanating from the crack tip and making use of Eq. (5) , the following expression has been obtained [64]:

$$\Delta K_{th} = 2\left[\frac{\rho\, bEd}{6\,\sigma_y}\right]^{(1+n'_b)/2} \cdot \sigma_y\sqrt{\pi d} \tag{8}$$

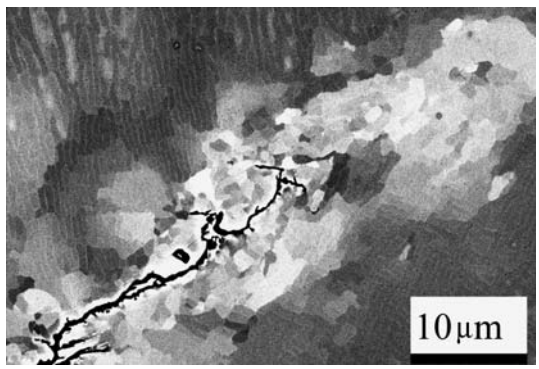

Fig. 6 Cell structure in the vicinity of fatigue crack and ahead of crack tip in conventional Cu CG polycrystal (electron channel contrast imaging -ECCI technique, courtesy of Dr. Y. Kaneko and Mr. M. Ishikawa, Osaka City University)

where b is the modulus of the Burgers vector, ρ is the density of mobile dislocations, E is the Young's modulus, n_b' is the cyclic hardening exponent, which is obtained from the cyclic stress-strain curve such as shown in Fig. 8 for UFG and CG copper. The cyclic stress-strain curve obeys commonly the power law:

$$\sigma_s = K_b'(\Delta\varepsilon_{pl}/2)^{n_b'} \quad (9)$$

with K_b'—the material's constant, σ_s and $\Delta\varepsilon_{pl}/2$—the cyclic saturation stress and plastic strain amplitude, respectively. Using Eq. (9) the curve fit of experimental data, Fig. 8, gives the n_b' value for UFG Cu to be of 0.2. We should emphasize that the cyclic hardening is quite pronounced in UFG Cu and the CSSC reveals considerably higher stress level than that of CG Cu of different grain sizes (the data for Cu having different grain sizes from [65, 66] are plotted in Fig. 8 for comparison). It is also worth noticing that the CSSC is virtually independent of the grain size for the CG material which in line with the introductory discussion above. Taking for Cu $E = 120$ GPa, $\sigma_y = 350$ MPa (Table 1), $d = 250$ nm and ρ close to $(1\div2) \times 10^{15}$ m^{-2} as is often reported in the literature [9] one obtains a reasonable estimate of ΔK_{th} of the order of 2 MPa $\times$ m$^{1/2}$, which compares favorably with data shown in Table 1. Nevertheless, this assessment should be regarded as qualitative because of considerable uncertainty in the dislocation density estimates. The significance of this model is that it accounts reasonably for the ΔK_{th} reduction with the grain size and highlights the importance of structural factors for the fatigue threshold. These factors include (i) the yield stress, (2) the susceptibility for cyclic hardening and (iii) mobile dislocation density. In line with this discussion it is worth noticing that although the magnitude in UFG is still smaller than that of CG materials, there is still considerable potential for its improvement due to a rather high n_b' cyclic hardening exponent value. Assuming the yield stress scaling with $\sqrt{\rho}$ the positive rather than negative influence of the increasing yield stress is expected on ΔK_{th} under the same grain size and cyclic hardening. The model can be used with some modification to account for the possible intergranular fatigue cracking in UFG metals due to excess grain dislocation density associated with non-equilibrium grain boundaries trapping and accommodating lattice dislocations during SPD, as illustrated schematically in Fig. 7.

Even though the some considerable differences in the microscopic details of the crack propagation may be noticed on the fracture surface and striation appearance in conventional fine-grained materials when compared to those in CG metals, grain size usually has little influence on the crack growth rate [3]. When the grain size is reduced down to submicrocrystalline region via SPD, the crack growth rate has been found higher than that in conventional metals, particularly in the near threshold region at relatively small ΔK [56]. Laird [67] supposed that microstructures hardened to maximum possible extent by cold-working may be susceptible to the cleavage mode of crack growth. Although SPD metals can be regarded as those "hardened to maximum possible extent", their remaining

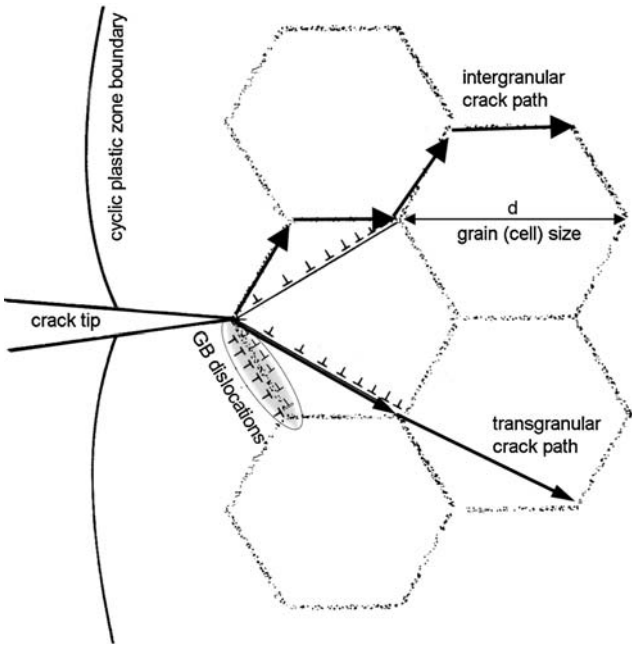

Fig. 7 Schematic illustration of the dislocation slip bands piled-up and blocked at the impenetrable grain (cell) boundary

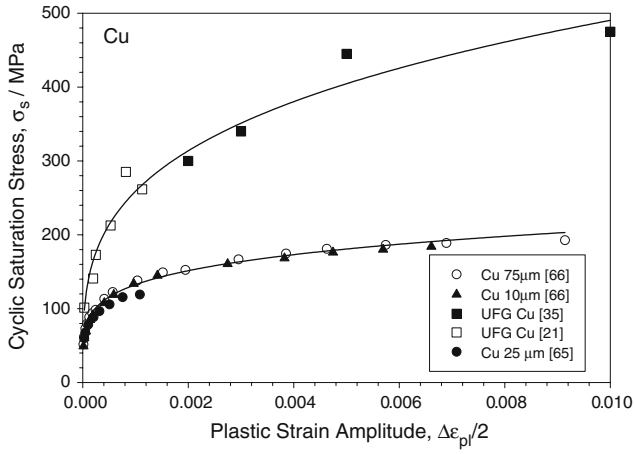

Fig. 8 Cyclic stress-strain curve for UFG and CG copper with different grain size

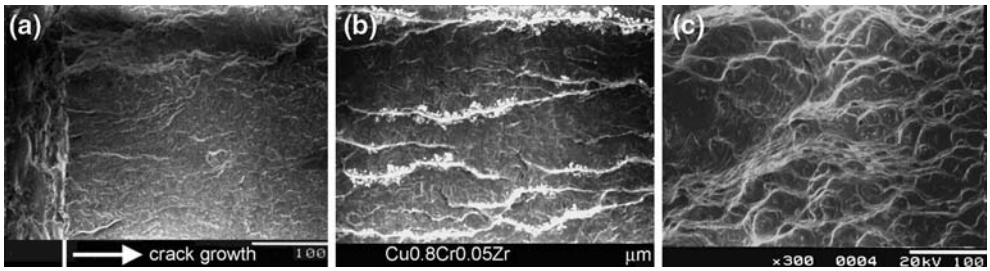

Fig. 9 Fragments of fatigue fracture surface of ECAP Cu0.8 Cr0.05Zr alloy: (**a**) low ΔK region corresponding to point A in Fig. 5, (**b**) intermediate ΔK region corresponding to point B in Fig. 5, (**c**) high Δ*K* region corresponding to point C in Fig. 5. An arrow indicates the crack growth direction

ductility is prominent enough so that the fatigue crack propagates in a rather ductile manner with visible striations corresponding to crack tip retardation and blunting as visible in Fig. 9, Fig. 10, Fig. 11. Similar striations associated with the position of the advancing crack front as a result of load variation are commonly observed in ordinary metals during fatigue crack growth under plane strain conditions (it is worth noticing that the striations are hardly visible generally under plane stress conditions). It has long been realized that the striations can render valuable information concerning crack propagation rates. Pelloux [68] has indicated that the microscopic crack growth rate, as measured by the striation spacing, is linearly proportional to the crack length. The stations with a broad variety of morphological features are also widely observed over the fatigue fracture surface of UFG ECAP metals, Figs. 9–11. No specific striation pattern which would be peculiar to the UFG metals solely are distinguished, indicating therefore that qualitatively similar description can be given to the crack growth in UFG and CG metals. Figures 9–10 show the fracture surface in Cu–0.8Cr–0.05Zr alloy after fatigue crack growth test in the CT specimen which has been cut normal to the extrusion direction and having a notch normal to the flow plane (sample ED in Fig. 5). Three regions corresponding to different magnitudes of ΔK are distinguishable. At high ΔK magnitude the ordinary dimple morphology is visible (Fig. 9c) similarly to observations in [53]. Although the stage I crack growth, cf. Fig. 4, 5 and Fig. 9a, in the near threshold region is usually confined to a few grains in CG materials provided that the cyclic plastic zone is smaller than the grain dimensions, the extent of this

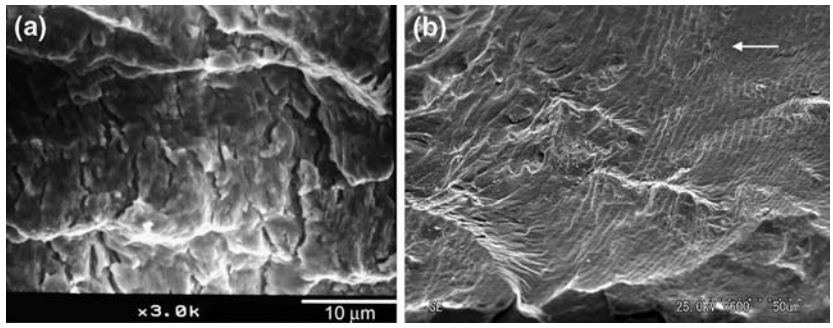

Fig. 10 Enlarged view of the fatigue fracture surface of ECAP Cu0.8Cr0.05Zr alloy: (**a**) corresponds to the first stage of crack growth, Fig. 9a; (**b**) corresponds to the second stage of crack growth, Fig. 9b

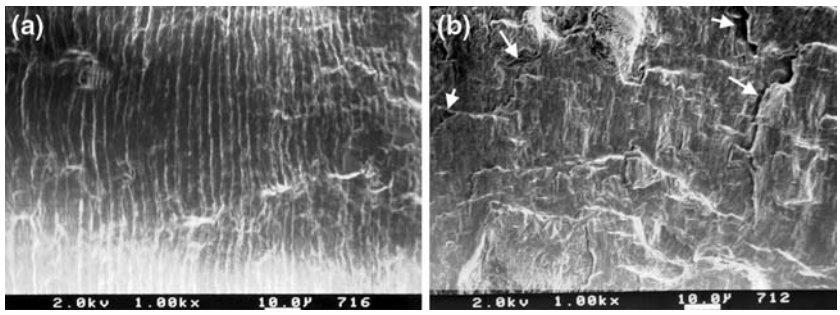

Fig. 11 Fragments of facture surface of ECAP Al3Mg0.2Sc alloy after HCF: (**a**) striations in the direction normal to the crack growth; (**b**) a view of the fracture surface where numerous microcracks and voids (indicated by arrows) can be seen along the fatigue crack path

stage in UFG metals is considerably greater than the grain size. This is not surprising since the size of the cyclic plastic zone in UFG metals is greater than the average grain size even at the lowest $\Delta K \approx \Delta K_{th}$. Ordinary regular striations are pronounced in UFG metals on the stage II crack growth regime) as shown in Fig. 9b, 10b and 11a.

In order to realize which factors control the crack growth resistance, it is instructive to examine the most common models of the crack growth. A very large number of models have been proposed to link the structure, mechanics of fracture, plastic deformation ahead of the crack tip and the crack growth rate. With some simplification, they can be classified into two groups [3]: crack tip plasticity models and damage accumulation models.

(i) Laird's general concept of crack tip blunting implies that fatigue crack propagation is controlled primarily by local plasticity near the crack tip. Evolving from the experimental observations of the correlation between the striation spacing with the crack growth rate (e.g., [66]), many models have been proposed to account for the crack behavior in ductile materials (see a comprehensive review by Suresh [3] and references therein). Since within the frames of linear fracture mechanics the crack tip opening displacement (CTOD) $\Delta\delta_t$ is related to the stress intensity factor, the crack growth rate is calculated in terms of ΔK

$$\frac{da}{dN} \approx \Delta\delta_t = \frac{(\Delta K_I)^2}{2\sigma_y' E} \tag{10}$$

With ordinary definition of ΔK by Eq.(4) this implies that da/dN is scaling with a. Regardless of precise mechanisms of crack behavior, all these theories are similar in their premise—crack growth occurs as a result of some local plastic deformation and, consequently, crack growth rate should be a function of the amount of slip ahead or in the intimate vicinity of the tip. Although data in Table 1 show that the crack growth rate da/dN in SPD-processed Cu and its alloys is nearly proportional to $(\Delta K)^2$, the inverse dependence on σ_y' is hardly expected: based on the CSSC shown in Fig. 8, one can find the σ_y' value in UFG Cu to be of 3 times higher than that in its CG counterpart, giving rise to the slower crack growth rate in the UFG state, which is not observed experimentally, Fig. 4.

Weertman [69] and Rice [70] proposed damage accumulation models of the crack growth in the form

$$\frac{da}{dN} \simeq \frac{(\Delta K)^4}{\mu\sigma_y^2 U^*} \tag{11}$$

where U^* is a hysteresis energy required per unit of newly created fatigue crack surface area. The latter expression implies explicitly that the Paris exponent equals to 4. The results of crack growth rate measurements summarized in Table 1 suggest that the fatigue cracks in Al-alloys grow primarily in the re-nucleation mode, i.e., in fair conformity with damage accumulation models. Indeed, Fig. 11 reveals numerous microcracks and voids created along the crack path in the ECAP AlMgSc alloy. Such a mechanism is quite common for many alloys containing local stress risers such as particles, inclusion, impurities, etc. Rather ductile UFG Cu and Cu-alloys however demonstrate the crack growth behavior controlled by local plasticity at the crack tip with m close to 2 as is advocated by the expression of type (10). Deviation from either 2 or 4 is naturally expected in many practical situations if we bear in mind that both mechanisms of crack growth can operate simultaneously.

Concluding this review, one can see that severe plastic deformation exerts a complex effect on the fatigue resistance. The enhancement of high cyclic fatigue life, which is often quantified by the endurance limit at small imposed plastic strains, can be naturally expected from the strength improvement after SPD. On the other hand, the resistance to fatigue crack growth, which is associated with relatively large cyclic strains and therefore with the ability of materials to deform plastically and uniformly, is found to be lower than that of polycrystals with conventional grain size. This finding however should not be too discouraging since the comparison has only been performed with annealed counterparts having much greater ductility. The ductility in the ultra-fine grain state, which can be gained in the course of optimized SPD with enhancing structural homogeneity and reducing local stress concentrators, is supposed to be the key factor for improving the crack growth resistance. Probable mechanisms responsible for both high cyclic fatigue life and crack resistance in ultra-fine grain materials have been discussed, though only qualitative discussion appeared to be possible from the data presently available.

As a guideline for future research, investigations are required regarding the fine structure in the vicinity of fatigue crack in UFG metals. The role of annealing and possibly bi-modal grain size distribution on fatigue limit, fatigue threshold and crack growth should be clarified. Precise characterization of crack nucleation mechanism under low applied cyclic strains is still lucking and is necessary for predictive modeling of fatigue crack resistance of UFG metals produced by SPD.

References

1. Segal VM, Reznikov VI, Drobyshevskiy AE, Kopylov VI (1981) Russ Metall 1:99
2. Segal VM (1995) Mater Sci Eng A197:157
3. Suresh S (1991) Fatigue of materials. Cambridge University Press
4. Mughrabi H (2000) In: Lowe TC, Valiev RZ (eds) Investigations and applications of severe plastic deformation, vol 3/80. NATO Science Series, Kluwer Publishers, p 241
5. Mughrabi H, Höppel HW, Kautz M (2004) Scripta Mater 51:807
6. Vinogradov A, Agnew S (2004) In: Schwarz JA, Contescu C, Putyera K (eds) Dekker encyclopedia of nanoscience and nanotechnology marcel dekker. Inc., USA, 2269
7. Höppel HW, Kautz M, Mughrabi H (2006) Proc. of 9th Int. Factigue Conference, Elsevier, FT207
8. Höppel HW, Mughrabi H, Vinogradov A (in press) In: Zehetbauer M, Zhu YT (eds) Bulk nanostructured materials. Wiley-VCH, Germany
9. Valiev RZ, Islamgaliev RK, Alexandrov IV (2000) Progr Mater Sci 45:103
10. Valiev RZ (2002) Nature 419:887
11. Wang Y, Chen M, Zhou F, Ma E (2002) Nature 419:912
12. Pelloux RM (1970) In: Burke JJ, Weiss V (eds) Ultrafine-grain metals. Syrakuse Univ. Press 231
13. Tompson AW, Backofen WA (1971) Acta metall 19:597
14. Lukáš P, Kunz L (1987) Mater Sci Eng 85:67
15. Winter AT (1974) Phil Mag 31:411
16. Kolobov YuR, Kashin OA, Sagymbaev EE, Dudarev EF, Bushnev LS, Grabovetskaya GP, Pochivalova GP, Girsova NV, Stolyarov VV (2000) Izvestiya VUZov, Fizika, 1:77 (in Russian)
17. Vinogradov A, Stolyarov VV, Hashimoto S, Valiev RZ (2001) Mater Sci Eng A 318:163
18. Mughrabi H, Wang R (1988) In: Lukáš P, Polák J (eds) Basic mechanisms in fatigue. Elsevier, Amsterdam, the Netherlands, p 1
19. Liang FL, Laird C (1989) Mater Sci Eng A 117:95
20. Plumtree A, Abdel-Raouf HA (2001) Int J Fatigue 23:177
21. Kunz L, Lukáš P, Svoboda M (2006) Mater Sci Eng A 424:97
22. Vinogradov A, Suzuki Y, Kopylov VI, Patlan V, Kitagawa K (2002) Acta metal 50:1636
23. Höppel HW, Mughrabi H (2001) Mat. Res. Soc. Symp. Proc. Vol. 634, Warrendale (PA): MRS, USA p. B 2.1.1
24. Stolyarov VV, Alexandrov IV, Kolobov YuR, Zhu M, Zhu T, Lowe T (1999) In: Wu XR, Wang ZG (eds) Fatigue'99, Proc. of the 7th Int. Fatigue Congress, vol 3. Beijing, P.R.China; Higher Education Press, P.R.China, 1999, p 1345
25. Turner NG, Roberts WT (1968) Trans AIME 242:1223
26. Gale WF, Totemeier TC (eds) (2004) Smitthells Metals Reference Book. Elsevier, Oxford, UK
27. Vinogradov A, Kopylov VI, Hashimoto S (2003) Mater Sci Eng A 355:277
28. Vinogradov A, Suzuki T, Hashimoto S, Kitagawa K, Kuznetsov A, Dobatkin S (2005) Mater Sci Forum 503–504:971
29. Vinogradov A, Ishida T, Kitagawa K, Kopylov VI (2005) Acta Mater 53:2181
30. Kitagawa K, Ishida T, Inoue A, Vinogradov A, Kopylov VI (2004) J JRICu 43:66 (in Japanese)
31. Lapovok R, Loader C, Dalla Torrea FH, Semiatin SL (2006) Mat Sci Eng A 425:36
32. Feltner CE, Laird C (1967) Acta metal 15:1621
33. Lukáš P, Kunz L (2002) Mater Sci Eng A 322:217
34. Vinogradov A, Patlan V, Kitagawa K (1999) Mater Forum 607:312
35. Vinogradov A, Hashimoto S (2001) Mat Trans JIM 42:74
36. Segal VM (1999) Mater Sci Eng A 271:322
37. Finney JM, Laird C (1975) Phil Mag 31:339
38. Laird C (1976) Mater Sci Eng 22:231
39. Buchinger L, Laird C (1985) Mater Sci Eng 76:71
40. Laird C, Buchinger L (1985) Metall Trans A 16A:2201
41. Ma B-T, Laird C (1989) Acta Metall 37:325
42. Essmann U, Gossele U, Mughrabi H (1981) Phil Mag A 44:405
43. Agnew SR, Vinogradov AYu, Hashimoto S, Weertman JR (1999) J Electronic Mater 28:1038
44. Höppel HW, Zhou ZM, Mughrabi H, Valiev RZ (2002) Phil Mag A 82:1781
45. Wu SD, Wang ZG, Jiang CB, Li GY (2002) Phil Mag Lett 82:559
46. Mughrabi H (1999) Fatigue Fract Eng Mater Struct 22:633
47. Kolobov YuR, Valiev RZ (eds) (2001) Grain boundary diffusion and properties of nano-structured materials. Nauka, Novosibirsk
48. Vinogradov A (2006) Mater Sci Forum 503–504:267
49. Höppel HW (2006) Mater Sci Forum 503–504:259
50. Yamasaki T, Miyamoto H, Mimaki T, Vinogradov A, Hashimoto S (2002) In: Zhu YT, Langdon TG, Mishra RS, Semiatin SL, Saran MJ, Lowe TC (eds) Ultrafine grain metals II. TMS, USA, p 361
51. Yamasaki T (2002) Ph.D. Thesis, Doshisha University, p 81
52. Higo Y, Pickard AC, Knott JF (1981) Metal Sci 15:233
53. Kiessling R, Hübner P, Biermann H, Vinogradov A (2006) Int J Mater Res 97:1566
54. Vinogradov A, Kitagawa K and Kopylov VI (2005) Mater Sci Forum 503–504:811
55. Chung CS, Kim JK, Kim HK, Kim WJ (2002) Mater Sci Eng A 337:39
56. Vinogradov A, Patlan V, Kitagawa K, Kawazoe M (1999) Nanostr Mater 11:925
57. Kim H-K, Choi M-I, Chung C-S, Shin DE (2003) Mater Sci Eng A 340:243
58. Muranaka K, Otake Y, Kitagawa K, Vinogradov A, Kopylov V (2005) J JRICu 44:291 (in Japanese)
59. Taira S, Tanaka K, Hoshina M (1979) In: Fong JT (ed) Fatigue mechanisms. ASTM STP 675, USA, p 165
60. Li X-D (1996) Theor Appl Fracture Mech 24:165
61. Lukáš P, Kunz L, Knesl Z, Weiss S, Stickler R (1985) Mater Sci Eng 70:91
62. Lukáš P, Kunz L (2002) Mater Sci Eng A 322:217
63. Huang HL, Ho NJ, Lin WB (2000) Mater Sci Eng A 279:261
64. Lukas JP, Gerberich WW (1983) Fatigue Eng Mater Struct 6:271
65. Mughrabi H, Wang R (1988) In: Lukáš P, Polák J (eds) Basic mechanisms in fatigue, academia. Prague and Elsevier Science Publ. Co. 1
66. Zhang J, Jiang Y (2006) Int J Plasticity 22:536
67. Laird C (1967) In: Fatigue crack propagation. ASTM STP 415, ASTM, p 131
68. Pelloux RM (1964) Trans Am Soc Metal 59:511
69. Weertman J (1966) Int J Fracture 2:460
70. Rice JR (1967) In: Fatigue Crack propagation. ASTM STP 415, ASTM, p 247